

# Generation of current mode filters using NAM expansion

Ahmed M. Soliman<sup>\*,†</sup>

*Electronics and Communication Engineering Department, Faculty of Engineering Cairo University, Egypt*

## SUMMARY

Systematic synthesis method to generate a family of current mode band-pass–low-pass circuits based on nodal admittance matrix (NAM) expansion is given. Eight equivalent circuits are obtained, five of them are new. Each of the generated circuits uses two grounded capacitors and three grounded resistors and two balanced output current conveyor (BOCCII) or two balanced output inverting current conveyor (BOICCI) or a combination of the two types. Generation of a low input impedance current mode band-pass–low-pass circuits based on NAM expansion results in 16 equivalent circuits. The NAM expansion is also used to generate 32 equivalent current mode universal filters using four BOCCII or BOICCI or a combination of the two types. Copyright © 2010 John Wiley & Sons, Ltd.

Received 26 May 2009; Revised 29 August 2009; Accepted 6 December 2009

**KEY WORDS:** nodal admittance matrix synthesis; nullator; norator; pathological current and voltage mirrors; balanced output current conveyors; balanced output inverting current conveyors

## 1. INTRODUCTION

The current mode filters are active circuits realizing current transfer functions. The ideal current mode filter should have very low input impedance and very high output impedance. It is also desirable to have grounded passive elements and independent control on the filter selectivity without affecting the radian frequency. Several current mode filters have been introduced in the literature [1–18]. A classification of current mode filters was published very recently in [7]. There is however no systematic generation method for most of the current mode filters available in the literature.

In this paper, a systematic generation method based on nodal admittance matrix (NAM) expansion is introduced. First families of band-pass–low-pass filters are generated, then family of current mode universal filters satisfying the ideality conditions of input and output impedance are also generated.

## 2. PATHOLOGICAL ELEMENTS AND NAM

Recently, a symbolic framework for systematic synthesis of linear active circuits based on NAM expansion was presented in [19, 20]. The matrix expansion process begins by introducing blank rows and columns, representing new internal nodes, in the admittance matrix. Then, nullators and norators are used to move the resulting admittance matrix elements to their final locations, properly describing either floating or grounded passive elements. The final NAM obtained includes finite elements representing passive circuit components.

<sup>\*</sup>Correspondence to: Ahmed M. Soliman, Electronics and Communication Engineering Department, Faculty of Engineering Cairo University, Egypt.

<sup>†</sup>E-mail: asoliman@ieee.org

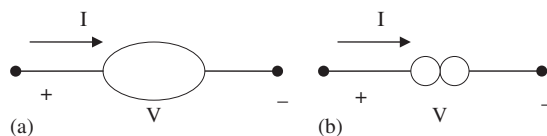


Figure 1. The nullor elements: (a) nullator and (b) norator.

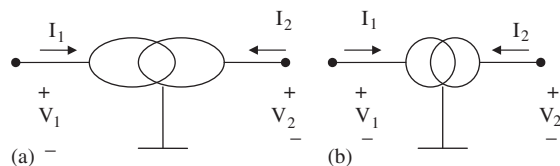


Figure 2. The mirror elements: (a) voltage mirror and (b) current mirror.

In this framework, nullators and norators [21] shown in Figure 1 ideally describe active elements in the circuit that are used. The nullator and norator are pathological elements that possess ideal characteristics and are specified according to the constraints they impose on their terminal voltages and currents. For the nullator  $V = I = 0$ , whereas the norator imposes no constraints on its voltage and current. A nullator–norator pair constitutes a universal active two-port network element called the nullor [21] and hence, nullator and norator are also called nullor elements. Additional pathological elements called mirror elements were introduced in [22, 23] to describe the voltage and current reversing actions. The voltage mirror (VM), shown in Figure 2(a), is a lossless two-port network element used to represent an ideal voltage reversing action and it is described by

$$V_1 = -V_2 \quad (1a)$$

$$I_1 = I_2 = 0 \quad (1b)$$

The current mirror (CM), shown in Figure 2(b), is a two-port network element used to represent an ideal current reversing action and it is described by

$$V_1 \text{ and } V_2 \text{ are arbitrary} \quad (2a)$$

$$I_1 = I_2 \text{ and they are also arbitrary} \quad (2b)$$

Although the CM element shown in Figure 2(b) has the same symbol as the regular CM, it is a bi-directional element and has a theoretical existence.

Very recently the systematic synthesis method based on NAM expansion and using nullor elements [19, 20] has been extended to accommodate mirror elements. This results in a generalized framework encompassing all pathological elements for ideal description of active elements [24–26]. Accordingly, more alternative realizations are possible and a wide range of active devices can be used in the synthesis.

It should be noted that after the synthesis procedure is completed the pathological elements are paired to realize the proper CCII or ICCII as follows:

The nullator and norator with a common terminal realize a CCII–.

The nullator and CM with a common terminal realize a CCII+.

The VM and norator with a common terminal realize an ICCII–.

The VM and CM with a common terminal realize an ICCII+.

In this paper, the systematic synthesis framework using NAM expansion is used to generate current mode second-order filters using current conveyors CCII [27] or inverting current conveyor (ICCI) [22] or combination of both types. First, a family of eight current mode band-pass–low-pass circuits using balanced output CCII (BOCCII) and balanced output ICCII (BOICCI) are

generated five of them are new. Next a family of 32 universal current mode filters using BOCCII and BOICCCII are also generated.

2.1. Formation of NAM equations

It is desirable to generate second-order current mode filters using the minimal number of passive elements necessary to provide independent control on the selectivity factor  $Q$  (namely two capacitors and three resistors) and using grounded passive elements.

Consider the denominator  $D(s)$  of the transfer function given by

$$D(s) = s^2 C_1 C_2 + s C_2 G_1 + G_2 G_3 \tag{3}$$

From Equation (3) there are two alternative equivalent NAM equations given by

$$Y = \begin{bmatrix} sC_1 + G_1 & -G_3 \\ G_2 & sC_2 \end{bmatrix} \tag{4}$$

This is defined as NAM type-A. The NAM Equation type-B is given by

$$Y = \begin{bmatrix} sC_1 + G_1 & G_3 \\ -G_2 & sC_2 \end{bmatrix} \tag{5}$$

3. GENERATION OF TYPE-A CURRENT MODE CIRCUITS

Four equivalent current mode filters realizing Equation (4) and using grounded passive elements are generated by expanding the NAM Equation (4) as given next.

Expanding the above matrix by adding a blank third row and third column, and adding a CM between nodes 1 and 3 in order to move  $-G_3$  from the 1, 2 position to 3, 2 position with positive sign, it follows that:

$$Y = \left. \begin{bmatrix} sC_1 + G_1 & 0 & 0 \\ G_2 & sC_2 & 0 \\ 0 & G_3 & 0 \end{bmatrix} \right\} \tag{6}$$

Adding a nullator between nodes 2 and 3 in order to move  $G_3$  to the diagonal position 3, 3 it follows that:

$$Y = \left. \begin{bmatrix} sC_1 + G_1 & \overbrace{0 \quad 0} \\ G_2 & sC_2 \quad 0 \\ 0 & 0 \quad G_3 \end{bmatrix} \right\} \tag{7}$$

Next a fourth blank row and column are added and  $G_2$  is moved to the diagonal position 4, 4 by adding a nullator between nodes 1 and 4 and a norator between nodes 2 and 4 as follows:

$$Y = \left. \begin{bmatrix} sC_1 + G_1 & 0 & 0 & 0 \\ 0 & sC_2 & 0 & 0 \\ 0 & 0 & G_3 & 0 \\ 0 & 0 & 0 & G_2 \end{bmatrix} \right\} \tag{8}$$

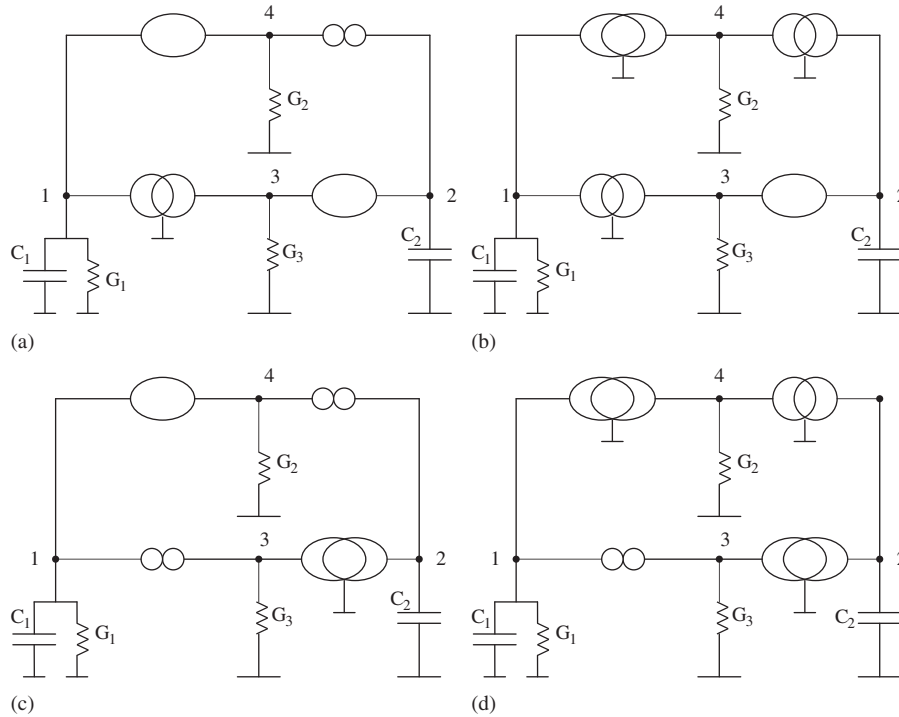


Figure 3. (a) Pathological representation of circuit A-1; (b) pathological representation of circuit A-2; (c) pathological representation of circuit A-3; and (d) pathological representation of circuit A-4.

Table I. Types of balanced output conveyors used in the circuit of Figure 5.

Circuit	Figure	Balanced output conveyor-1 ( $Z_1, Z_2$ )	Balanced output conveyor-2 ( $Z_1, Z_2$ )	BP sign	LP sign	Reference
A-1	3(a)	BOCCII ( $Z-, Z+$ )	BOCCII ( $Z+, Z-$ )	+	+	3
A-2	3(b)	BOICCII ( $Z+, Z-$ )	BOCCII ( $Z+, Z-$ )	+	+	New
A-3	3(c)	BOCCII ( $Z-, Z+$ )	BOICCII ( $Z-, Z+$ )	+	+	New
A-4	3(d)	BOICCII ( $Z+, Z-$ )	BOICCII ( $Z-, Z+$ )	+	+	4
B-1	4(a)	BOCCII ( $Z+, Z-$ )	BOCCII ( $Z-, Z+$ )	-	+	3
B-2	4(b)	BOICCII ( $Z-, Z+$ )	BOCCII ( $Z-, Z+$ )	-	+	New
B-3	4(c)	BOCCII ( $Z+, Z-$ )	BOICCII ( $Z+, Z-$ )	-	+	New
B-4	4(d)	BOICCII ( $Z-, Z+$ )	BOICCII ( $Z+, Z-$ )	-	+	New

The above NAM equation is represented in Figure 3(a) which is realizable using a CCII+ and a CCII-. Adding a second Z terminal to each of the two CCII and injecting the input current at node 1 results in a two BOCCII as given in Table I.

The NAM Equation (4) can also be expanded as follows:

$$Y = \left[ \begin{array}{cccc} sC_1 + G_1 & 0 & 0 & 0 \\ 0 & sC_2 & 0 & 0 \\ 0 & 0 & G_3 & 0 \\ 0 & 0 & 0 & G_2 \end{array} \right] \quad (9)$$

Figure 3(b) realizes the above equation; the corresponding a BOICCII and a BOCCII is described in Table I.

The NAM Equation (4) can also be expanded as follows:

$$Y = \begin{bmatrix} sC_1 + G_1 & 0 & 0 & 0 \\ 0 & sC_2 & 0 & 0 \\ 0 & 0 & G_3 & 0 \\ 0 & 0 & 0 & G_2 \end{bmatrix} \quad (10)$$

Figure 3(c) realizes the above equation; the corresponding a BOCCII and a BOICCCII is described in Table I.

The fourth alternative NAM expansion for Equation (4) is given by:

$$Y = \begin{bmatrix} sC_1 + G_1 & 0 & 0 & 0 \\ 0 & sC_2 & 0 & 0 \\ 0 & 0 & G_3 & 0 \\ 0 & 0 & 0 & G_2 \end{bmatrix} \quad (11)$$

Figure 3(d) realizes the above equation; the corresponding a BOCCII and a BOICCCII is described in Table I. Circuits A-1 and A-4 have been reported before [3, 4] and the other two circuits are new.

#### 4. GENERATION OF TYPE-B CURRENT MODE CIRCUITS

The NAM Equation (5) can be expanded and will result in four additional current mode circuits classified as type-B circuits.

Adding third blank row and column to Equation (5) and connecting a nullator between nodes 2 and 3 and a norator between nodes 1 and 3 to move  $G_3$  to the diagonal position 3, 3, it follows that:

$$Y = \begin{bmatrix} sC_1 + G_1 & 0 & 0 \\ -G_2 & sC_2 & 0 \\ 0 & 0 & G_3 \end{bmatrix} \quad (12)$$

Next adding a fourth blank row and column and connecting a nullator between nodes 1, 4 and a CM between nodes 2 and 4 to move the  $-G_2$  to the diagonal position 4, 4 with positive sign it follows that:

$$Y = \begin{bmatrix} sC_1 + G_1 & 0 & 0 & 0 \\ 0 & sC_2 & 0 & 0 \\ 0 & 0 & G_3 & 0 \\ 0 & 0 & 0 & G_2 \end{bmatrix} \quad (13)$$

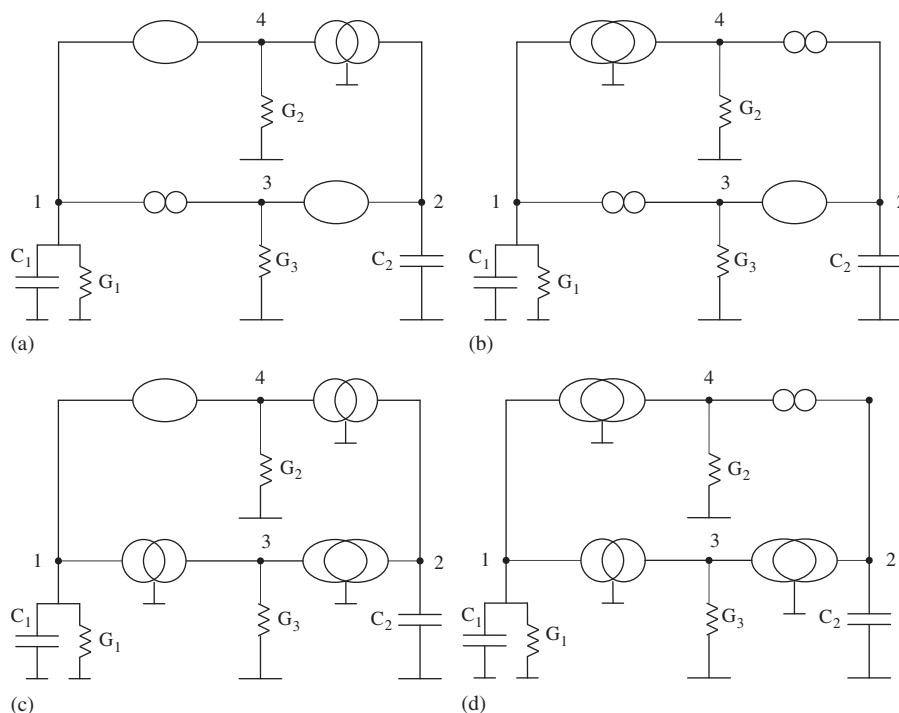


Figure 4. (a) Pathological representation of circuit B-1; (b) pathological representation of circuit B-2; (c) pathological representation of circuit B-3; and (d)-pathological representation of circuit B-4.

Figure 4(a) realizes the above equation which is realizable using a CCII+ and a CCII-. Adding a second Z terminal to each of the two CCII and injecting the input current at node 1 results in a two BOCCII as given in Table I.

The NAM Equation (5) can also be expanded as follows:

$$Y = \begin{bmatrix} sC_1 + G_1 & 0 & 0 & 0 \\ 0 & sC_2 & 0 & 0 \\ 0 & 0 & G_3 & 0 \\ 0 & 0 & 0 & G_2 \end{bmatrix} \quad (14)$$

Figure 4(b) realizes the above equation which is realizable by a BOCCII and a BOICCI as given in Table I.

The NAM Equation (5) can also be expanded as follows:

$$Y = \begin{bmatrix} sC_1 + G_1 & 0 & 0 & 0 \\ 0 & sC_2 & 0 & 0 \\ 0 & 0 & G_3 & 0 \\ 0 & 0 & 0 & G_2 \end{bmatrix} \quad (15)$$

Figure 4(c) realizes the above equation which is realizable by a BOCCII and a BOICCI as given in Table I.

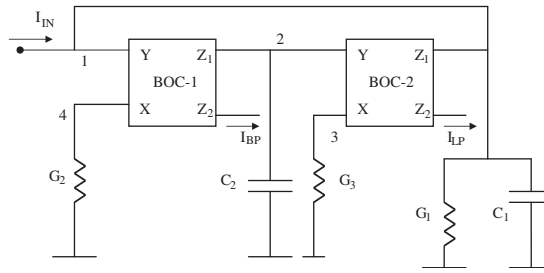


Figure 5. Current mode filter realizing the eight pathological circuits.

The NAM Equation (5) can also be expanded as follows:

$$Y = \begin{bmatrix} sC_1 + G_1 & 0 & 0 & 0 \\ 0 & sC_2 & 0 & 0 \\ 0 & 0 & G_3 & 0 \\ 0 & 0 & 0 & G_2 \end{bmatrix} \quad (16)$$

Figure 4(d) realizes the above equation which is realizable by two BOIC-1 as given in Table I. The transfer functions for each of the eight circuits are given by

$$\frac{I_{BP}}{I_{IN}} = \frac{\pm sC_2 G_2}{s^2 C_1 C_2 + sC_2 G_1 + G_2 G_3} \quad (17)$$

$$\frac{I_{LP}}{I_{IN}} = \frac{G_2 G_3}{s^2 C_1 C_2 + sC_2 G_1 + G_2 G_3} \quad (18)$$

From the above equations, therefore

$$\omega_0 = \sqrt{\frac{G_2 G_3}{C_1 C_2}}, \quad Q = \frac{1}{G_1} \sqrt{\frac{C_1 G_2 G_3}{C_2}} \quad (19)$$

$$\text{BP gain } (\omega_0) = \frac{G_2}{G_1} \quad (20)$$

The magnitude of the DC gain of the low-pass filter is unity. The band-pass polarity is non-inverting in the type A and inverting in the type-B circuits. The low-pass polarity is non-inverting in both types of filters.

From Equation (19) it is seen that the passive sensitivities are all less than or equal to 1. The lowest is the frequency sensitivity with respect to  $R_1$  which is zero and the highest is the  $Q$  sensitivity with respect to  $R_1$  which is 1. Figure 5 represents the generalized configuration realizing the pathological circuits of Figures 3 and 4.

### 5. LOW INPUT IMPEDANCE BP-LP FILTERS

As stated in the introduction the ideal current mode filter should have a very low input impedance. In this section it is shown how to generate 16 equivalent current mode band-pass-low-pass filter circuits eight of them belong to type A and the other eight circuits belong to type B.

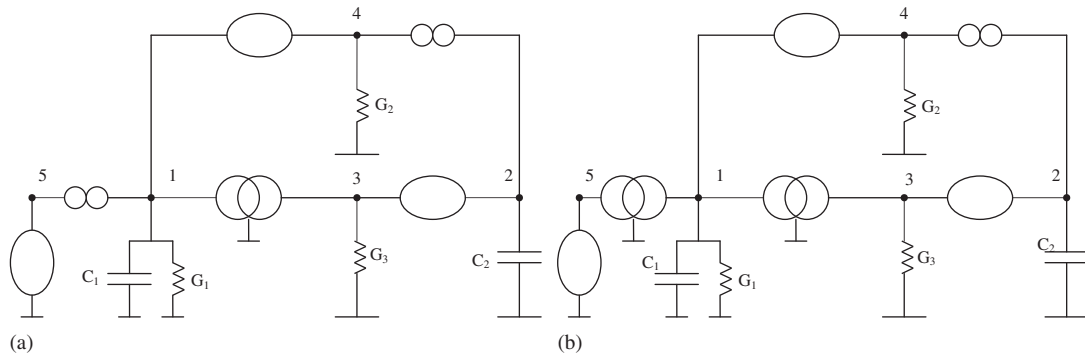


Figure 6. (a) Type A-1 filter using CCII- as input stage and (b) Type A-1 filter using CCII+ as input stage.

Consider the NAM Equation (8) and adding a fifth row and column and using infinity parameters representing the additional CCII-, thus

$$Y = \begin{bmatrix} sC_1+G_1 & 0 & 0 & 0 & \infty_1 \\ 0 & sC_2 & 0 & 0 & 0 \\ 0 & 0 & G_3 & 0 & 0 \\ 0 & 0 & 0 & G_2 & 0 \\ 0 & 0 & 0 & 0 & -\infty_1 \end{bmatrix} \quad (21)$$

The above equation is represented by pathological elements as shown in Figure 6(a). The current mode filter in this case employs a first stage acting as a current follower and the band-pass and low-pass polarities are both non-inverting as in the circuit A-1.

Alternatively the NAM can be expanded as follows:

$$Y = \begin{bmatrix} sC_1+G_1 & 0 & 0 & 0 & \infty_1 \\ 0 & sC_2 & 0 & 0 & 0 \\ 0 & 0 & G_3 & 0 & 0 \\ 0 & 0 & 0 & G_2 & 0 \\ 0 & 0 & 0 & 0 & \infty_1 \end{bmatrix} \quad (22)$$

The current mode filter in this case employs a first stage acting as a current inverter as shown in Figure 6(b) and the band-pass and low-pass polarities are both inverting opposite to the previous case.

Next consider the NAM Equation (9) and adding a fifth row and column and using infinity parameters representing the additional CCII- thus

$$Y = \begin{bmatrix} sC_1+G_1 & 0 & 0 & 0 & \infty_1 \\ 0 & sC_2 & 0 & 0 & 0 \\ 0 & 0 & G_3 & 0 & 0 \\ 0 & 0 & 0 & G_2 & 0 \\ 0 & 0 & 0 & 0 & -\infty_1 \end{bmatrix} \quad (23)$$

The above equation can be represented by pathological elements as demonstrated before. The current mode filter in this case employs a first stage acting as a current follower and the band-pass and low-pass polarities are both non-inverting as in the circuit of Figure 3(b).

Alternatively the NAM can be expanded as follows:

$$Y = \begin{bmatrix} sC_1+G_1 & 0 & 0 & 0 & \infty_1 \\ 0 & sC_2 & 0 & 0 & 0 \\ 0 & 0 & G_3 & 0 & 0 \\ 0 & 0 & 0 & G_2 & 0 \\ 0 & 0 & 0 & 0 & \infty_1 \end{bmatrix} \quad (24)$$

The current mode filter in this case employs a first stage acting as a current inverter and the band-pass and low-pass polarities both inverting opposite to the previous case.

Next consider the NAM Equation (10) and adding a fifth row and column and using infinity parameters representing the additional CCII- thus

$$Y = \begin{bmatrix} sC_1+G_1 & 0 & 0 & 0 & \infty_1 \\ 0 & sC_2 & 0 & 0 & 0 \\ 0 & 0 & G_3 & 0 & 0 \\ 0 & 0 & 0 & G_2 & 0 \\ 0 & 0 & 0 & 0 & -\infty_1 \end{bmatrix} \quad (25)$$

The above equation is represented by pathological elements as demonstrated before. The current mode filter in this case employs a first stage acting as a current follower and the band-pass and low-pass polarities are both non-inverting as in the circuit of Figure 3(c).

Alternatively the NAM can be expanded as follows:

$$Y = \begin{bmatrix} sC_1+G_1 & 0 & 0 & 0 & \infty_1 \\ 0 & sC_2 & 0 & 0 & 0 \\ 0 & 0 & G_3 & 0 & 0 \\ 0 & 0 & 0 & G_2 & 0 \\ 0 & 0 & 0 & 0 & \infty_1 \end{bmatrix} \quad (26)$$

The current mode filter in this case employs a first stage acting as a current inverter and the band-pass and low-pass polarities both inverting opposite to the previous case.

Next consider the NAM Equation (11) and adding a fifth row and column and using infinity parameters representing the additional nullor or CCII-, thus

$$Y = \begin{bmatrix} sC_1+G_1 & 0 & 0 & 0 & \infty_1 \\ 0 & sC_2 & 0 & 0 & 0 \\ 0 & 0 & G_3 & 0 & 0 \\ 0 & 0 & 0 & G_2 & 0 \\ 0 & 0 & 0 & 0 & -\infty_1 \end{bmatrix} \quad (27)$$

The above equation can be represented by pathological elements as demonstrated before. The current mode filter in this case employs a first stage acting as a current follower and the band-pass and low-pass polarities are both non-inverting as in the circuit of Figure 3(d).

Alternatively the NAM can be expanded as follows:

$$Y = \begin{bmatrix} sC_1+G_1 & 0 & 0 & 0 & \infty_1 \\ 0 & sC_2 & 0 & 0 & 0 \\ 0 & 0 & G_3 & 0 & 0 \\ 0 & 0 & 0 & G_2 & 0 \\ 0 & 0 & 0 & 0 & \infty_1 \end{bmatrix} \quad (28)$$

The current mode filter in this case employs a first stage acting as a current inverter and the band-pass and low-pass polarities both inverting opposite to the previous case.

Similarly eight more circuits can be generated from the two stage type-B filters by adding a current follower or a current inverter stage at the input to achieve the desirable very low input impedance.

It should be noted that all of the 16 reported three stage conveyor circuits can compensate the effects of the parasitic  $R_X$  and  $C_Z$  by subtracting the value of  $R_{X2}$  from  $R_2$ ,  $R_{X3}$  from  $R_3$ ,  $C_{Z2}$  from  $C_2$  and  $(C_{Z1} + C_{Z3})$  from  $C_1$ . The only parasitic element affecting the circuit is  $R_{X1}$  which results in finite input resistance equal to  $R_{X1}$  which depends on the CMOS or bipolar circuit of the current follower or inverter used.

### 6. GENERATION OF UNIVERSAL CURRENT MODE FILTERS

In this section generation of universal current mode filters based on NAM expansion are considered. Thirty two current mode universal circuits are generated based on NAM expansion, four of the circuits employ BOCCII and a similar four circuits employ BOICCII, the remaining 24 new circuits employ combination of BOCCII and BOICCII.

To limit the paper length only the four BOCCII circuits are included. The first circuit is obtained from Equation (5) and the NAM expansion is given by:

$$Y = \begin{bmatrix} sC_1 & 0 & 0 & 0 & 0 & \infty_1 \\ 0 & sC_2 & 0 & 0 & 0 & 0 \\ 0 & 0 & G_3 & 0 & 0 & 0 \\ 0 & 0 & 0 & G_2 & 0 & 0 \\ 0 & 0 & 0 & 0 & G_1 & 0 \\ 0 & 0 & 0 & 0 & 0 & \infty_1 \end{bmatrix} \quad (29)$$

It is seen that both brackets and infinity parameters are used together.

The infinity parameters in the sixth column represent a CM between nodes 1 and 6 and a nullator between nodes 6 and ground representing the input stage of the current mode filter shown in Figure 7(a). The input current is injected at node 6 and the circuit is realized by four CCII+, adding a second Z- output to each of the CCII+ the four BOCCII circuit shown in Figure 8(a) is obtained. The circuit equations are given by

$$\frac{I_{HP}}{I_{IN}} = \frac{s^2 C_1 C_2}{s^2 C_1 C_2 + s C_2 G_1 + G_2 G_3} \quad (30)$$

$$\frac{I_{BP1}}{I_{IN}} = \frac{s C_2 G_2}{s^2 C_1 C_2 + s C_2 G_1 + G_2 G_3} \quad (31)$$

$$\frac{I_{BP2}}{I_{IN}} = \frac{s C_2 G_1}{s^2 C_1 C_2 + s C_2 G_1 + G_2 G_3} \quad (32)$$

$$\frac{I_{LP}}{I_{IN}} = \frac{G_2 G_3}{s^2 C_1 C_2 + s C_2 G_1 + G_2 G_3} \quad (33)$$

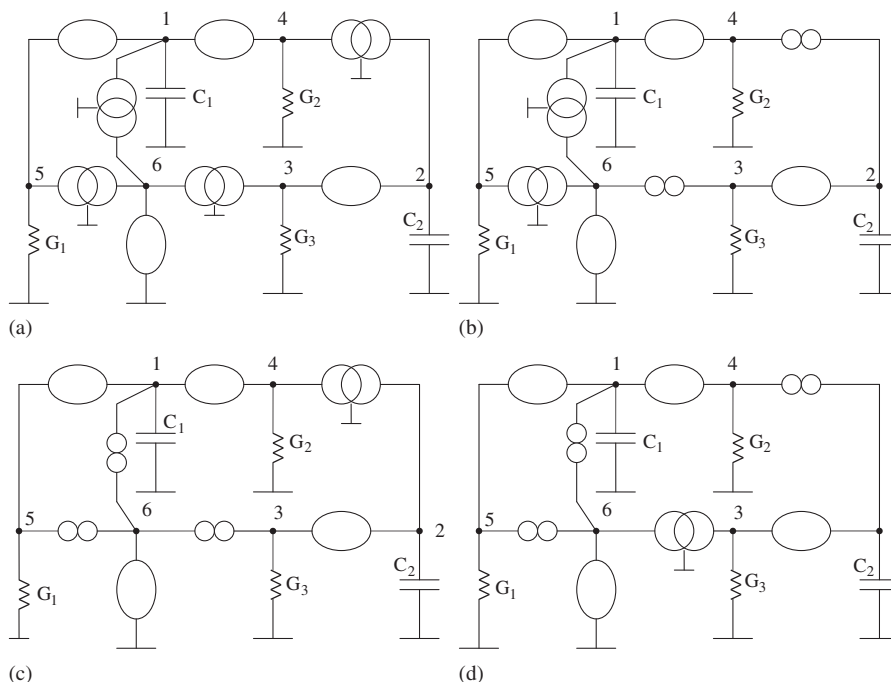


Figure 7. (a) Pathological representation of universal current mode filter 1; (b) pathological representation of universal current mode filter 2; (c) pathological representation of universal current mode filter 3; and (d) pathological representation of current mode filter 4.

The second current mode filter is obtained from Equation (4) and the NAM equation is given by:

$$Y = \begin{bmatrix} sC_1 & 0 & 0 & 0 & 0 & \infty_1 \\ 0 & sC_2 & 0 & 0 & 0 & 0 \\ 0 & 0 & G_3 & 0 & 0 & 0 \\ 0 & 0 & 0 & G_2 & 0 & 0 \\ 0 & 0 & 0 & 0 & G_1 & 0 \\ 0 & 0 & 0 & 0 & 0 & \infty_1 \end{bmatrix} \quad (34)$$

Figure 7(b) represents the pathological realization of the above equation and Figure 8(b) represents the four BOCCII current mode filters. The circuit equations are the same as the previous circuit except the band-pass polarity is inverting.

The third current mode filter is obtained from Equation (5) and the NAM equation is given by:

$$Y = \begin{bmatrix} sC_1 & 0 & 0 & 0 & 0 & \infty_1 \\ 0 & sC_2 & 0 & 0 & 0 & 0 \\ 0 & 0 & G_3 & 0 & 0 & 0 \\ 0 & 0 & 0 & G_2 & 0 & 0 \\ 0 & 0 & 0 & 0 & G_1 & 0 \\ 0 & 0 & 0 & 0 & 0 & -\infty_1 \end{bmatrix} \quad (35)$$

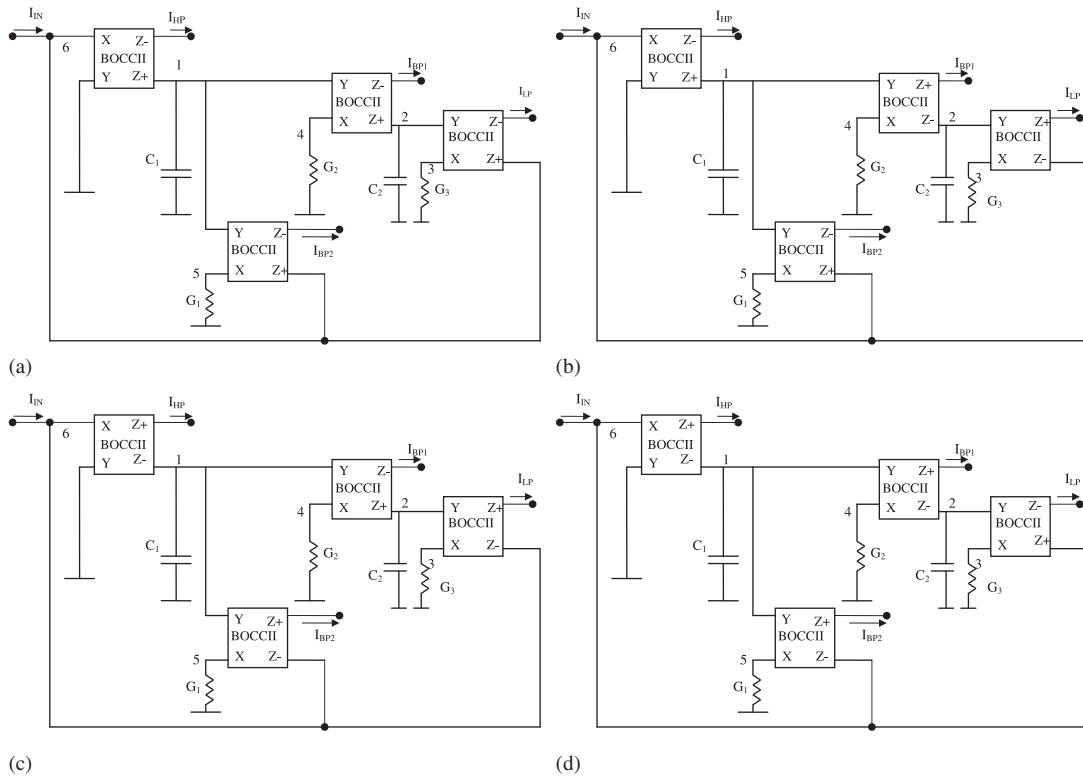


Figure 8. (a) Universal current mode filter 1; (b) universal current mode filter 2; (c) universal current mode filter 3; and (d) universal current mode filter 4.

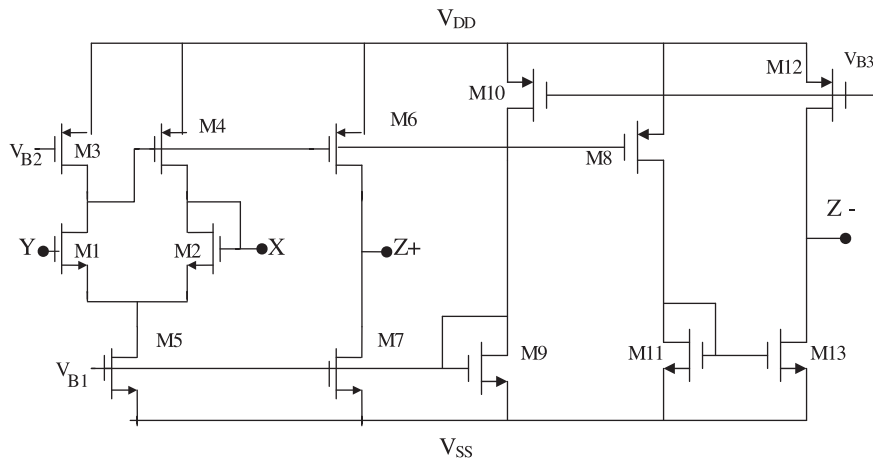


Figure 9. CMOS circuit of the balanced output CCII [28].

Figure 7(c) represents the pathological realization of the above equation and Figure 8(c) represents the four BOCCII current mode filters. The circuit equations are the same as the previous circuit except the high-pass and the band-pass polarities are inverting.

The fourth current mode filter is obtained from Equation (4) and the NAM equation is given by:

$$Y = \begin{bmatrix} sC_1 & 0 & 0 & 0 & 0 & \infty_1 \\ 0 & sC_2 & 0 & 0 & 0 & 0 \\ 0 & 0 & G_3 & 0 & 0 & 0 \\ 0 & 0 & 0 & G_2 & 0 & 0 \\ 0 & 0 & 0 & 0 & G_1 & 0 \\ 0 & 0 & 0 & 0 & 0 & -\infty_1 \end{bmatrix} \quad (36)$$

Figure 7(d) represents the pathological realization of the above equation and Figure 8(d) represents the four BOCCII current mode filters. The circuit equations are the same as the previous circuit except the high-pass polarity is inverting.

It should be noted that in realizing all-pass transfer functions the second bandpass  $I_{BP2}$  with inverting polarity should be used so that the realizable all-pass will have independent control on  $Q$  by varying  $G_1$ .

The parasitic elements that are affecting the circuits are  $C_{Z3}$ ,  $C_{Z4}$  and  $R_{X1}$  and the input current is affected by first-order low-pass filter [29] at the input resulting in the following expression for the actual input current  $I'$  entering port X of the input stage:

$$I' = I \frac{1}{1 + s[C_{Z3} + C_{Z4}]R_{X1}} \quad (37)$$

The other parasitic elements are compensated by subtracting their values from circuit design values as follows. The parasitic resistances  $R_{X2}$ ,  $R_{X3}$  and  $R_{X4}$  are subtracted from  $R_2$ ,  $R_3$  and  $R_1$ , respectively. The parasitic capacitances  $C_{Z1}$  and  $C_{Z2}$  are subtracted from  $C_1$  and  $C_2$ , respectively.

## 7. SIMULATION RESULTS

Spice simulation results using technology SCN 05 feature size  $0.5\mu\text{m}$  from MOSIS vendor: AGILENT. Figure 9 represents the CMOS circuit of a balanced output CCII [28] with  $V_{DD} = 1.5\text{V}$ ,  $V_{SS} = -1.5\text{V}$ ,  $V_{B1} = -0.56\text{V}$ ,  $V_{B2} = 0.172\text{V}$ ,  $V_{B3} = 0.2\text{V}$ . Transistor aspect ratios are given in Table II.

The circuit of Figure 8(a) is simulated to have  $f_o = 1\text{MHz}$  and  $Q = 0.707$  for low-pass maximally flat magnitude response. The circuit design parameters taken are  $C_1 = C_2 = 100\text{PF}$ ,  $R_3 = R_2 = 1.59\text{k}\Omega$ ,  $R_1 = 1.124\text{k}\Omega$ .

Figure 10(a) represents the magnitude and phase characteristics together with the ideal response. It is seen that the simulated results are close to the ideal responses. Simulations for the circuits of Figures 8 (b)–(d) are carried out and the magnitude and phase frequency responses are shown

Table II. Aspect ratios of the balanced output CCII of Figure 9.

Transistor	W(mm)/L(mm)
M1,M2	20/1
M3	50/2.5
M4,M6,M8	80/2.5
M5	100/2.5
M7,M9,M11,M13	50/2.5
M10,M12	100/2.5

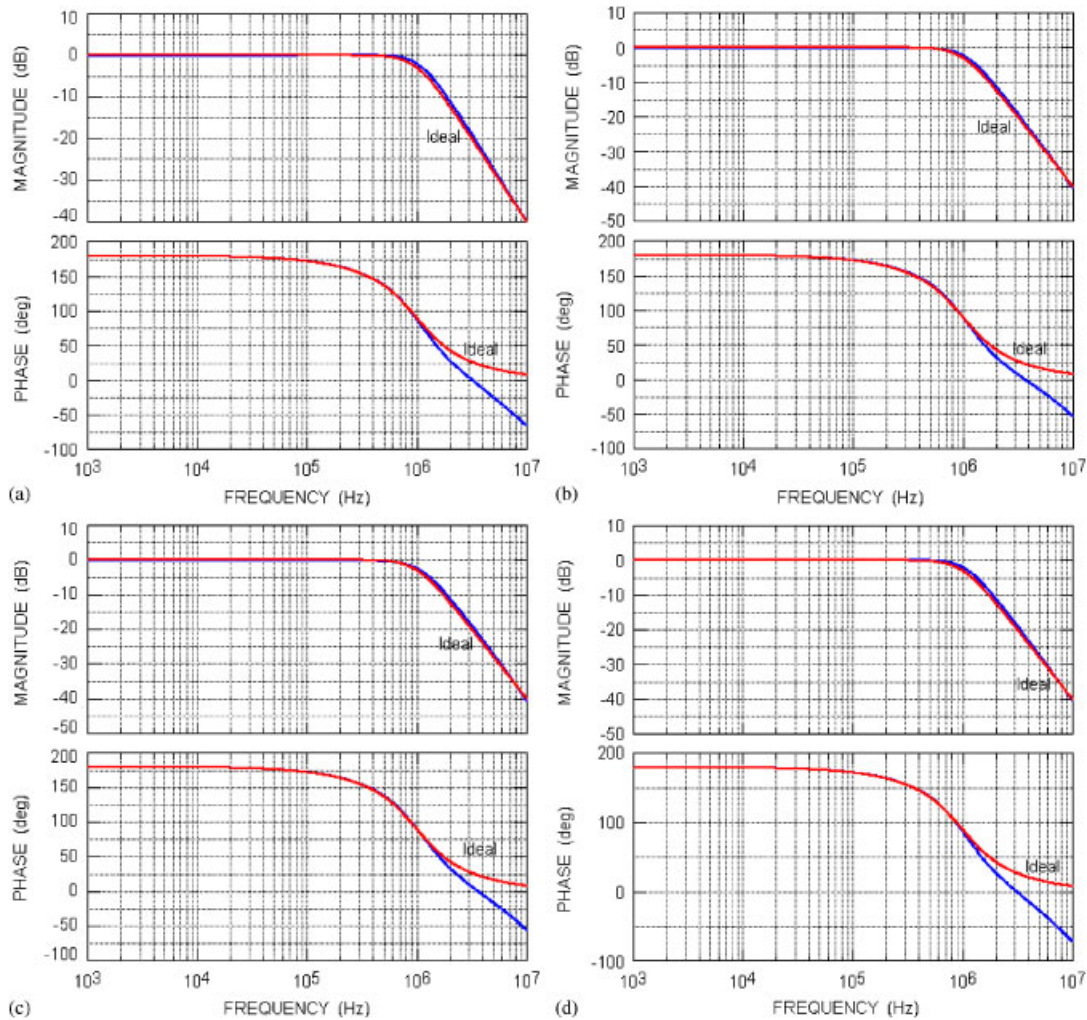


Figure 10. (a) Low-pass frequency response universal filter 1; (b) low-pass frequency response universal filter 2; (c) low-pass frequency response universal filter 3; and (d) low-pass frequency response universal filter 4.

in Figures 10 (b)–(d). The total power dissipation for the four filter circuits are given respectively by 8.58288 mW, 11.4332 mW, 11.0251 mW and 10.3237 mW. It is seen that filter 1 has the smallest power dissipation.

Figure 11 represents the simulated noise voltage at the low-pass current output node when terminated by 1 k $\Omega$  load resistor. It is seen that filter 1 has the smallest output noise.

## 8. CONCLUSIONS

The NAM expansion method using nullor elements and pathological mirrors is used to generate 16 grounded passive element conveyor based current mode band-pass–low-pass filters. The generation of 32 universal current mode filters is also demonstrated using NAM expansion. This is the first article up to the author knowledge that uses NAM expansion in the generation of current

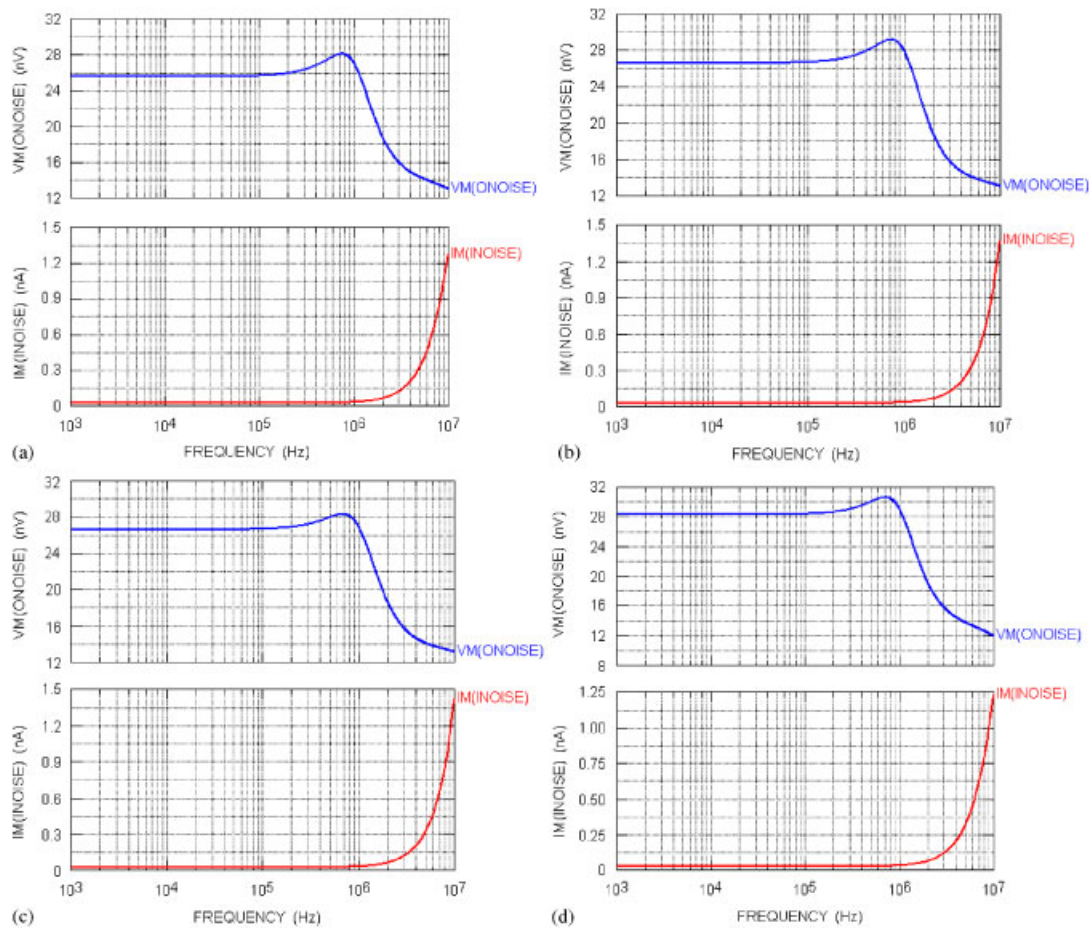


Figure 11. (a) Simulation of output noise for filter 1; (b) simulation of output noise for filter 2; (c) simulation of output noise for filter 3; and (d) simulation of output noise for filter 4.

mode filters. Simulation results for four of the universal current mode filters are included showing close frequency responses to the ideal case.

#### REFERENCES

1. Soliman AM. Generation of CCII and CFOA filters from passive RLC filters. *International Journal of Electronics* 1998; **85**:293–312.
2. Chang CM. Universal Active current filter with single input and three outputs using CCII's. *Electronics Letters* 1993; **29**:1932–1933.
3. Soliman AM. New current mode filters using current conveyors. *International Journal of Electronics and Communications (AEU)* 1997; **51**:275–278.
4. Soliman AM. New grounded capacitor current mode bandpass lowpass filters using two balanced output ICCII. *Journal of Active and Passive Electronic Devices* 2008; **3**:175–184.
5. Soliman AM. Current mode universal filter. *Electronics Letters* 1995; **31**:1420–1421.
6. Soliman AM. Current mode filters using two output inverting CCII. *International Journal of Circuit Theory and Applications* 2008; **36**:875–881.
7. Soliman AM. Current mode universal filters using current conveyors: classification and review. *Journal of Circuits Systems and Signal Processing* 2008; **27**:405–427.
8. Soliman AM. Voltage mode and current mode Tow Thomas bi-quadratic filters using ICCII. *International Journal of Circuit Theory and Applications* 2007; **35**:463–467.
9. Hwang YS, Wu DS, Chen JJ, Shih CC, Chou WS. Design of current-mode MOSFET-C filters using OTRAs. *International Journal of Circuit Theory and Applications* 2008; **36**:397–411.
10. Souliotis G, Haritantis I. Current-mode filters based on current mirror arrays. *International Journal of Circuit Theory and Applications* 2008; **36**:173–183.

11. Horng JW, Hou CL, Chang CM. Multi-input differential current conveyor, CMOS realization and application. *IET Circuits, Devices and Systems* 2008; **2**:469–475.
12. Lee SS, Zele RH, Allstot DJ, Liang G. A Continuous-Time Current-Mode Integrator. *IEEE Transactions on Circuits and Systems* 1991; **38**:1236–1238.
13. Sanchez-Sinencio E, Geiger RL, Nevarez-Lozano H. Generation of continuous-time two integrator loop OTA filter structures. *IEEE Transactions on Circuits and Systems* 1988; **35**:936–946.
14. Chang CM. Universal active current filter with three inputs and one output using plus type CCII. *Electronic Letters* 1997; **33**:1207–1208.
15. Higashimura M. Current mode transfer function using CCII with grounded passive elements. *IEICE Transactions* 1991; **74**:1017–1019.
16. Papazoglou CA, Karybakas CA. Non-interacting electronically tunable CCII based current mode bi-quadratic filters. *IEE Proceedings on Circuits, Devices and Systems* 1997; **144**:178–184.
17. Wang HY, Lee CT. Versatile insensitive current mode universal bi-quad implementation using current conveyors. *IEEE Transactions on Circuits and Systems II* 2001; **48**:409–413.
18. Wu J, El-Masry E. Current mode ladder filters using multiple output current conveyors. *IEE Proceedings on Circuits Devices and Systems* 1996; **143**:218–222.
19. Haigh DG, Tan FQ, Papavassiliou C. Systematic synthesis of active-RC circuit building-blocks. *Analog Integrated Circuits and Signal Processing* 2005; **43**(3):297–315.
20. Haigh DG, Clarke TJW, Radmore PM. Symbolic framework for linear active circuits based on port equivalence using limit variables. *IEEE Transactions on Circuits and Systems I* 2006; **53**(9):2011–2024.
21. Carlin HJ. Singular network elements. *IEEE Transactions on Circuit Theory* 1964; **11**:67–72.
22. Awad IA, Soliman AM. Inverting second-generation current conveyors: the missing building blocks, CMOS realizations and applications. *International Journal of Electronics* 1999; **86**:413–432.
23. Awad IA, Soliman AM. On the voltage mirrors and the current mirrors. *Analog Integrated Circuits and Signal Processing* 2002; **32**:79–81.
24. Saad RA, Soliman AM. Use of mirror elements in the active device synthesis by admittance matrix expansion. *IEEE Transactions on Circuits and Systems I* 2008; **55**(9):2726–2735.
25. Saad RA, Soliman AM. Generation modeling and analysis of CCII-Based gyrators using the generalized symbolic framework for linear active circuits. *International Journal of Circuit Theory and Applications* 2008; **36**(3):289–309.
26. Saad RA, Soliman AM. A new approach for using the pathological mirror elements in the ideal representation of active devices. *International Journal of Circuit Theory and Applications* 2010; **38**(2):148–178.
27. Sedra AS, Smith KC. A second generation current conveyor and its applications. *IEEE Transactions on Circuit Theory* 1970; **132**:132–134.
28. Palmisano G, Palumbo G. A simple CMOS CCII+. *International Journal of Circuit Theory and Applications* 1995; **23**:599–603.
29. Fabre A, Saaid O, Barthelemy H. On the frequency limitations of circuits based on second generation current conveyors. *Analog Integrated Circuits and Signal Processing* 1995; **7**:113–129.